Journal of Theoretical and Applied Physics (2020) 14:159–169
https://doi.org/10.1007/s40094-020-00372-7

RESEARCH

In vitro bioactivity of silicophosphate glasses doped with ZnO, SrO or CuO

H. A. ElBatal[1] · A. A. El-Kheshen[1] · M. A. Marzouk[1] · N. A. Ghoneim[1] · F. H. ElBatal[1] · M. A. Ouis[1] · A. M. Fayad[1] · A. M. Abdelghany[2]

Received: 24 January 2020 / Accepted: 6 March 2020 / Published online: 20 March 2020

Abstract
Silicophosphate glasses with variable divalent ion dopants (Zn^{2+}, Sr^{2+} or Cu^{2+}) were prepared via melt annealing route. Parent and doped glasses were thermally heat-treated through a two-step regime to be converted into their glass–ceramic derivatives. Fourier transform infrared (FT-IR) spectral data were recorded for parent glasses and their glass–ceramics derivatives to identify the structural building units which reveal vibrational bands due to both main phosphate and some silicate groups and to verify the bioactivity behavior after immersion in diluted phosphate solution. X-ray diffraction studies indicate the formation of different phosphate and silicate crystalline phases in the derived glass–ceramics which varied with the type of dopant oxide. SEM investigations of the glass–ceramics before and after immersion in phosphate solution showed multi-component microcrystalline textures in the studied micrographs before immersion. Nodular-shaped microcrystalline features were identified after immersion in phosphate solution referring to the formation of crystalline hydroxyapatite. The undoped glass–ceramic is identified to crystallize in almost equal silicate and phosphate phases, while with the dopant ZnO, SrO or CuO, the crystalline phases are only of phosphates, while the silicate phase is assumed to be retained in the surrounding remaining vitreous boundaries.

Keywords Silicophosphate · Glass · Glass–ceramics · ZnO · CuO · SrO · Bioactivity

Introduction

It has been realized and accepted that the function of biomaterials is directed to replace diseased or damaged tissues (including bones) [1, 2]. The first generation of biomaterials was early selected to be as bioinert as possible and thereby minimize the formation of scar tissue at the interface of host tissues. Metals and polymers that were early designed and applied as bioinert materials triggered fibrous encapsulation after implantation, rather than forming a stable interface or strong chemical bond with tissues. The invention of bioactive glasses in 1969–1971 provided for the first time an alternative as the second generation, interfacial bonding of an implant with host tissues and reported to be able to stimulate more bone regeneration than other bioactive ceramics [1, 2]. Hench introduced in his review article in 1998 [3] some of the clinically used bioactive ceramics including bioglasses, glass–ceramics and ceramics mostly of silicate and phosphate compositions together with some composites for various applications.

Many authors [4, 5] have extended the promising studies by Day et al. [6, 7] for the usefulness of various borate glasses as efficient biomaterials with their rapid dissolution and nearly complete conversion to the basic bonding hydroxyapatite when immersed in phosphate solution, Also, later subsequent studies include the search to incorporate trace elements with the bioglasses or glass–ceramics to act as therapeutic or antimicrobial candidates [8, 9].

The present study comprises the preparation of some silicophosphate glasses based on the basic chemical composition P_2O_5 (60)–Na_2O(20)–SiO_2(10)–CaO(10) together with samples containing added dopants of either 2%ZnO, 2%SrO or 1% CuO. These dopants have been found to induce favorable properties for the biomaterials [1–5, 9].

✉ A. M. Abdelghany
a.m_abdelghany@yahoo.com

[1] Glass Research Department, National Research Centre, 33 El Bohouth St. (former EL Tahrir), Dokki, Giza 12622, Egypt

[2] Spectroscopy Department, Physics Division, National Research Centre, 33 ElBohouth St., (Former El-Tahrir St.) Dokki, Giza 12622, Egypt

The investigations include multiple characterizations of the glasses and glass–ceramic derivatives prepared by two-step controlled thermal heat treatment of the parent glasses. FT infrared absorption spectra of the glasses and glass–ceramics were carried out before and after immersion in phosphate solution for 2 weeks. Also, scanning electron microscopic studies of the surfaces of the two varieties (glasses and glass–ceramics) were done before and after immersion. X-ray diffraction patterns were identified for the glass–ceramics to find out the separated crystalline phases upon thermal heat treatment.

Presented work expected to identify the main structural building units in both the glasses and glass–ceramics and their variations in response to crystallization or upon immersion in phosphate solution. The role of divalent dopants (Zn^{2+}, Sr^{2+}, Cu^{2+}) on the bioactivity or bone-bonding was studied.

Experimental details

Preparation of the glasses

The batches of the glasses were prepared from chemically pure laboratory chemicals including sodium dihydrogen orthophosphate (NaH_2PO_4), purified pulverized quartz and calcium carbonate, and the dopants were added in the form of ZnO, $SrCO_3$ and CuO.

The weighed batches were melted in covered porcelain crucibles at 1150 °C for 90 min with occasional rotating the melts at intervals of 30 min to reach complete mixing and homogeneity. The finished melts were poured into pre-heated stainless steel molds with the dimensions required. The prepared glassy samples were immediately transferred to an annealing muffle furnace regulated at 250 °C. After 1 h, the muffle was switched off and left to cool to room temperature at a rate of 30 °C/h with the prepared glasses inside.

The details of the chemical compositions are depicted in Table 1.

Table 1 Chemical composition of the prepared glass samples

Glass no.	Wt%				Added oxide
	P_2O_5	SiO_2	CaO	Na_2O	
1	60	10	10	20	0
2	60	10	10	20	2%ZnO
3	60	10	10	20	1%CuO
4	60	10	10	20	2%SrO

Controlled thermal heat treatment (preparation of the corresponding glass–ceramics)

The original parent glasses were heat-treated in a special muffle with a heating rate of 5 °C/min to 285 °C first selected temperature deduced from DTA and thermal expansion measurements (nucleation temperature) held at this temperature for 6 *h* necessary to produce sufficient nuclei sites. Afterward, the muffle was raised to the second temperature for completing the growth at 420 °C and held at this temperature for 3 *h*. The muffle was then switched off and left to cool to room temperature at a rate of 30 °C/h.

Structural FTIR spectral analysis for glasses and corresponding glass–ceramics

The identification of the structural building groups for both glasses and glass–ceramics was done by measuring their FT infrared absorption spectra within the wavenumber range 4000–400 cm^{-1} using a recording FT infrared spectrometer (type Mattson 5000, USA). The KBr disk technique was adopted using fine powders of the glasses or glass–ceramics. The IR measurements were immediately taken after preparing the disks to avoid moisture attack for the powders. The same IR absorption measurements were repeated after the immersion of the powders in a diluted phosphate solution for 2 weeks.

Morphological studies using scanning electron microscopic technique (SEM)

The surfaces of both the glasses and glass–ceramics were examined by the SEM apparatus model (Philips XL, 30 attached with EDX unit, accelerating voltage 30 kV). All samples were coated with a thin film of gold for morphological examinations.

X-ray diffraction analysis

The separated crystalline phases within the glass–ceramic derivatives were examined as a fine powder using X-ray diffractometer type (Philips PW 1390 type) adopting Ni-filter and Cu-target.

Results

DTA and thermal expansion coefficient studies

Figures 1 and 2 illustrate the DTA and thermal expansion data of the base undoped glass. The obtained data from these

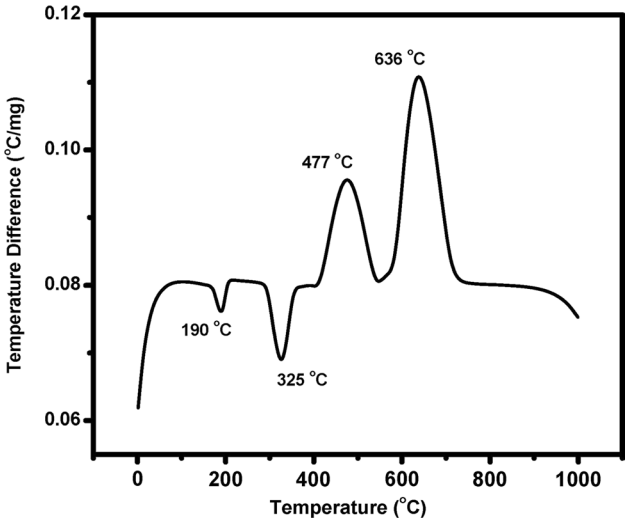

Fig. 1 DTA pattern of the base glass

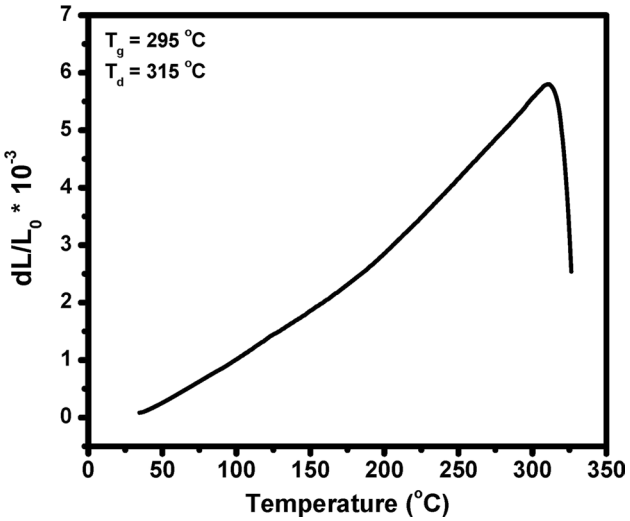

Fig. 2 Thermal expansion behavior of the base glass

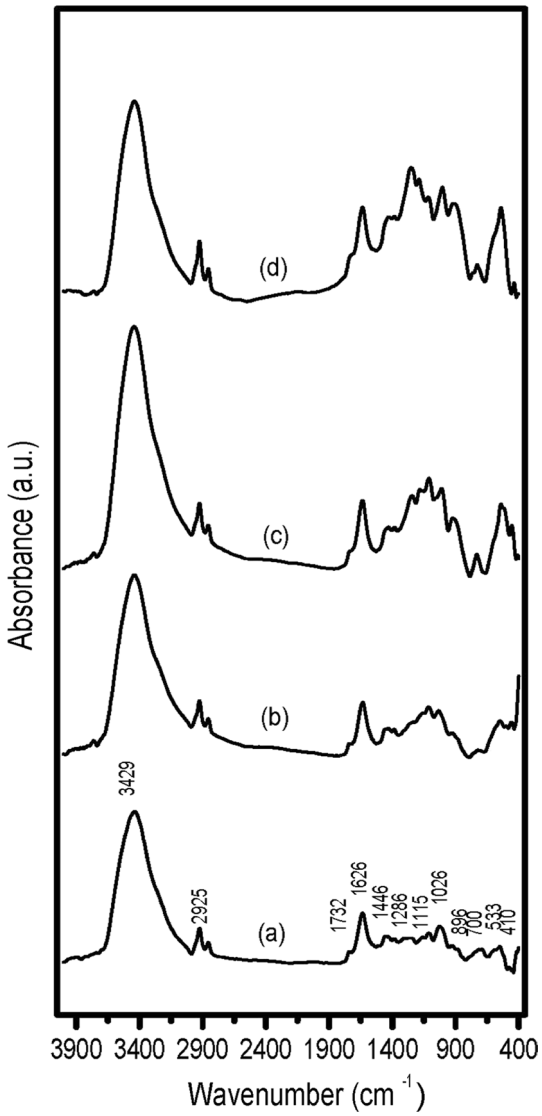

Fig. 3 FTIR spectra of the studied glasses before immersion in phosphate solution, **a** base glass, **b** glass containing ZnO, **c** glass containing CuO and **d** glass containing SrO

techniques were used to detect the suitable heating regime for converting glass samples to their corresponding glass ceramic derivatives.

FT infrared absorption spectra of the studied glasses and glass–ceramics before immersion

The FTIR spectra of the prepared glasses are illustrated in Fig. 3, and the spectral details reveal condensed or composite IR peaks within the mid-region (400–1700) cm^{-1}. It is, therefore, necessary to make a deconvolution process for the obtained composite IR spectra to behave to identify hidden or overlapped bands due to the presence of two composing structural groups (PO_4 and SiO_4). The IR deconvoluted spectrum of the base undoped soda–lime silicophosphate glass in Fig. 4 reveals the following spectral details:

(a) The far-IR region shows five successive peaks at about 428, 505, 702 and 785 cm^{-1}.
(b) The mid-region extending from about 800 to 1700 cm^{-1} reveals eight peaks at about 872, 1030, 1102, 1285, 1390, 1460, 1627 and 1685 cm^{-1}.
(c) The near-IR region extending from about 2750 to 4000 cm^{-1} shows two peaks at 2846 and 2925 cm^{-1} followed by a very broad and strong band extending from about 3000 to 3750 cm^{-1} and revealing a central peak at about 3443 cm^{-1}.

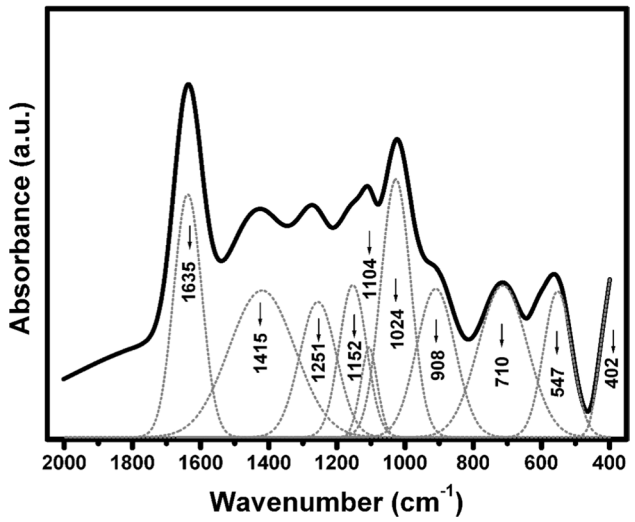

Fig. 4 Deconvoluted FTIR spectrum of base glass (no. a) before immersion in phosphate solution

The other doped-glasses reveal nearly similar condensed IR absorption peaks within the same mid-regions but showing limited variable intensities of the peaks.

Figure 5 illustrates the FTIR spectra of the glass–ceramic derivatives before immersion in phosphate solution. Careful inspection of the FTIR spectra indicates that the vibrational bands of the glass–ceramics are also concentrated within the wavenumber range 400–1700 cm^{-1} and the peaks are quite stronger and sharper than their parent glasses but generally are in the same wavenumber vibrational sites. The near-IR

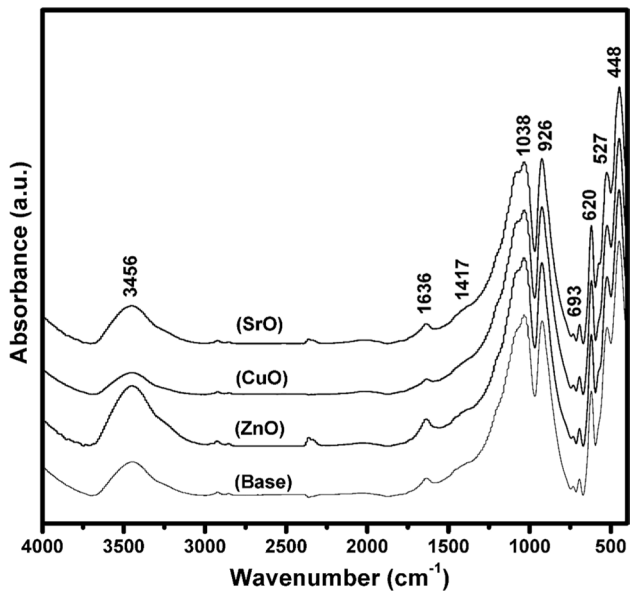

Fig. 5 FTIR absorption spectra of glass–ceramic derivatives before immersion

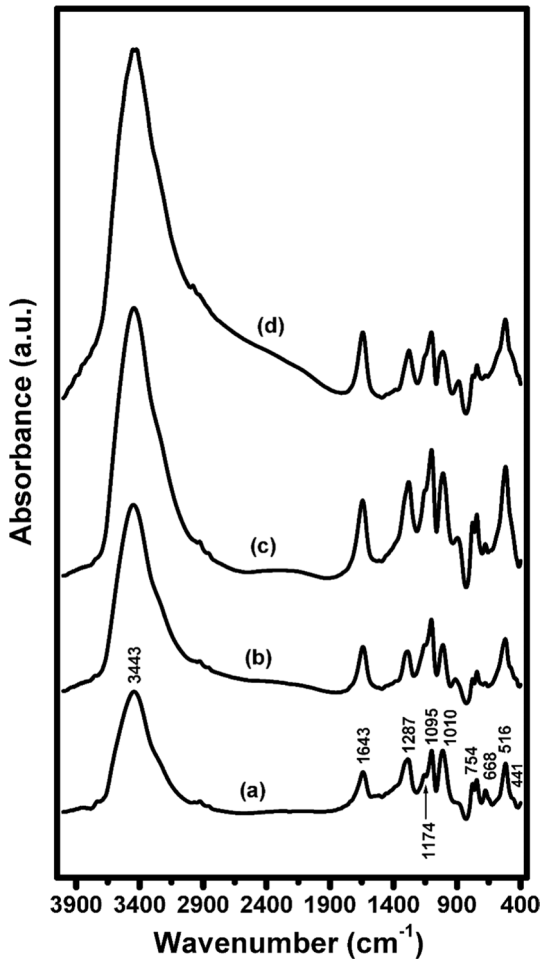

Fig. 6 FTIR spectra of glasses after immersion in phosphate solution for 2 weeks, **a** base glass, **b** glass containing ZnO, **c** glass containing CuO and **d** glass containing SrO

peaks within the range 390–3700 cm^{-1} are lower in intensities than their parent glasses.

Figure 6 shows the FTIR spectra of the studied glasses after immersion in phosphate solution for 2 weeks. The IR spectra are generally similar to the IR spectra before immersion, and the vibrational peaks within the range 400–1700 cm^{-1} are more identified and revealing peaks at 441, 516, 666, 754, 1010, 1095, 1174, 1287 and 1643 cm^{-1}. The most important spectral features which represent the effects of immersion seem to cause variations in the spectral results. The response of the reactions between the constituents of the glasses including major phosphate ions and some silicate ions with the immersion solution is leading to the appearance of far-IR peaks around 515–750 cm^{-1}. The near IR most prominent and broadband centered at about 3440 cm^{-1} is quite distinctive as before immersion.

Figure 7 reveals the FTIR spectra of samples from prepared glass–ceramic derivatives after immersion in phosphate solution for 2 weeks. The IR spectra of

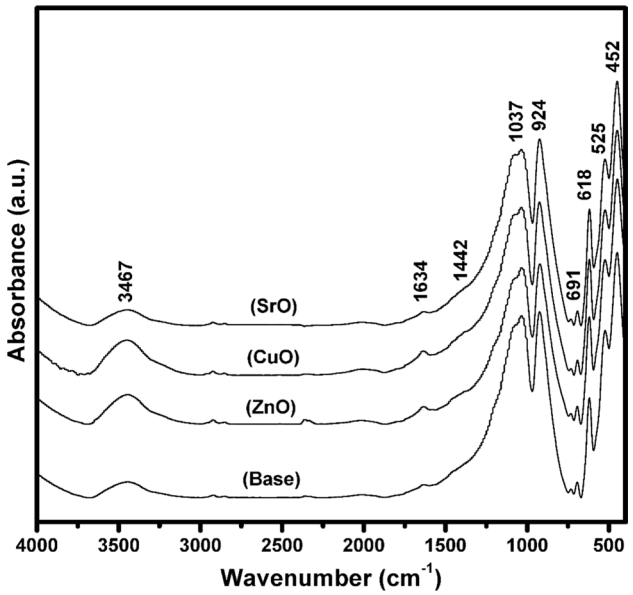

Fig. 7 FTIR absorption spectra of glass–ceramic derivatives after immersion in phosphate solution for 2 weeks

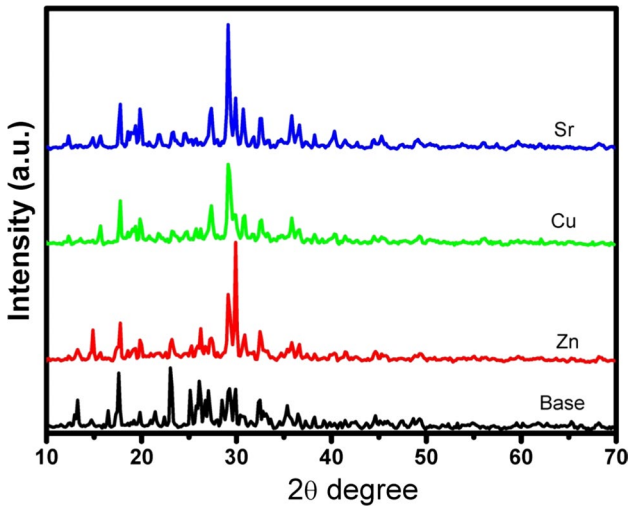

Fig. 8 XRD pattern of glass–ceramic samples

the glass–ceramics after immersion are similar to that before immersion including the distinctive appearance of the mid-IR peaks within 400–1600 cm^{-1} and the lower intensity of the near-IR broadband than that for the parent glasses. Careful examination of Figs. 5 and 7 indicates that the glass–ceramics show high intense and sharp vibrational peaks and they seem to be stable immersion in phosphate solution.

X-ray diffraction patterns of the studied glass–ceramics

Figure 8 illustrates the X-ray diffraction patterns of the four crystalline glass–ceramic derivatives. The detailed separated crystalline phases after thermal heat treatment of the parent glasses are summarized as follows:

(a) The base undoped glass–ceramic reveals six crystalline phases arranged as follows: (1) sodium calcium silicate $Na_2Ca_3Si_6O_{16}$ (card no. 77-0386c) with 28.7%, (2) sodium hydrogen phosphate (Na $5H_2(PO_4)$ (P_2O_7) card no. 77-0096) with 25.1%, (3) sodium phosphate $Na_3P_3O_9$ (card no. 72-6386(C) with 24.8%), (4) wollastonite $CaSiO_3$ card no. 76-0186(C) with 10.9% and (5) grumantite $Na(Si_2O_4)(OH)H_2O$ card no. 77-0983 with 5.3%-suolunite $CaSiO_3H_2O$ card no. 74-2248 (C) with 5.1%.

(b) The glass–ceramic doped with ZnO shows three crystalline phases: (1) calcium phosphate oxide $Ca_4(PO_4)26$ card no. 70-1379(C) with 45.2%, (2) zinc phosphate $Zn_3(PO_4)_2$ card no. 36-1489(*) with 33.9% and (3) sodium phosphate $Na_3P_3O_9$ card no. 72-1628 with 20.9%.

(c) The glass–ceramic doped with CuO reveals four crystalline phases: (1) sodium hydrogen phosphate with 40.0%, (2) calcium phosphate oxide with 33.6%-pseudomalachite $(Cu_5(PO_4)_2(OH)_4$ card no. 72-1678(C) with 15.2% and (3) copper hydrogen phosphate $(CuHPO_3(H_2O)_2$ card no. 72-1367(C) with 11.2%

(d) The glass–ceramic doped with SrO shows five crystalline phases: (1) sodium hydrogen phosphate with 33.7%, (2) calcium phosphate oxide with 28.3%-sodium phosphate with 22.4%, (3) sodium phosphate hydrate $(NaPO_3$ $4(H_2O)$ card no. 76-2279-with 11.7% and (4) sodium strontium phosphide $(Na_2Sr_3P_4)$ with 3.8%

Scanning electron microscopic investigations

Figure 9a, b illustrates the morphological features of the four glass–ceramics before and after immersion in phosphate solution. The photomicrographs reveal the following textural features:

(a) The undoped glass–ceramic shows almost microcrystalline ellipsoidal texture with interlocking vitreous remnants between the microcrystals after immersion. The microcrystalline features are smaller with some rounded microcrystals scattered within the texture.

(b) The glass–ceramic doped with ZnO shows hemispherical texture with gathering microcrystals with a residual vitreous matrix. After immersion, the whole texture is

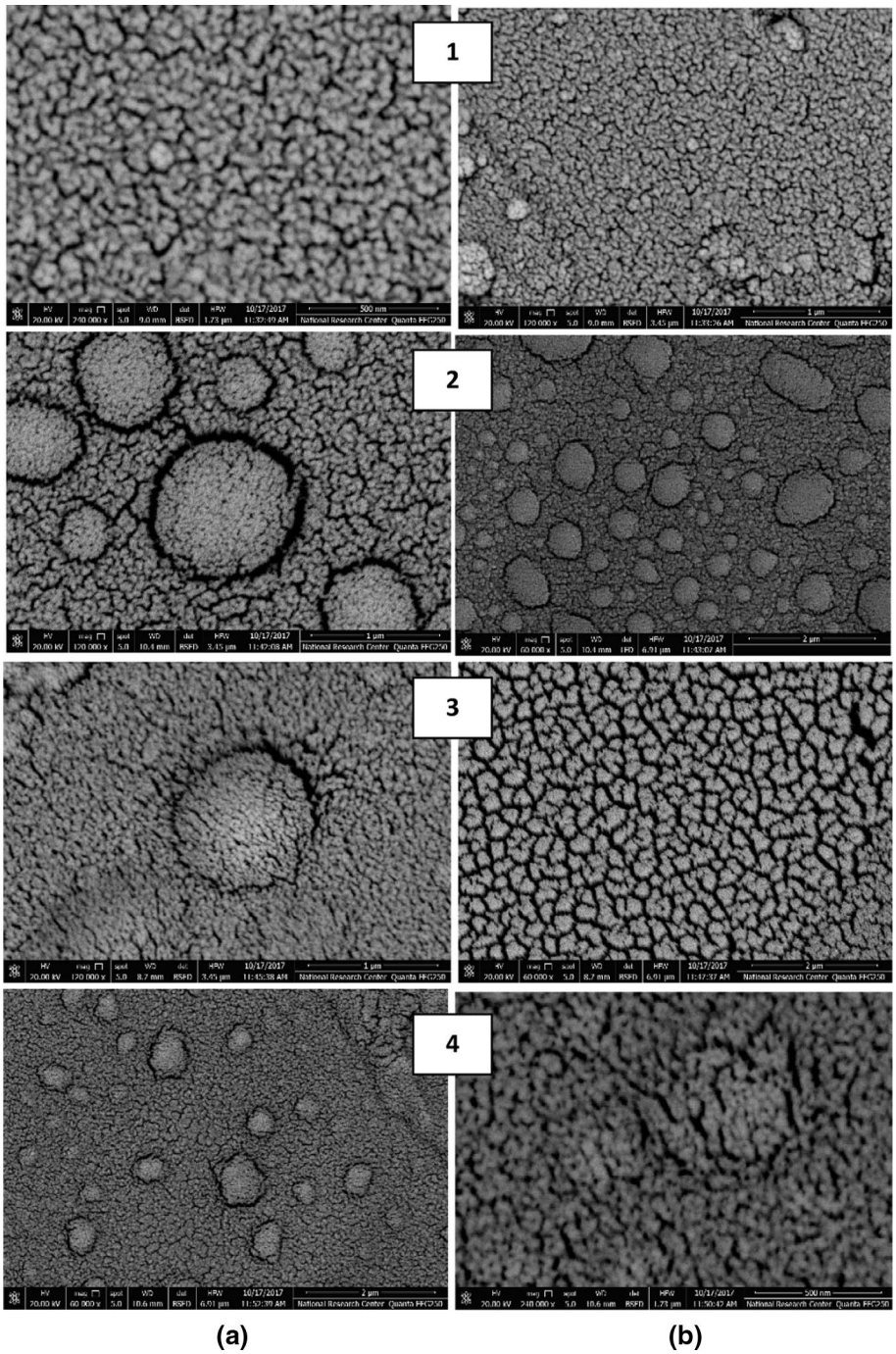

Fig. 9 SEM micrographs of glass ceramics samples before and after immersion in phosphate solution for 2 weeks, 1: base glass–ceramic, 2: glass–ceramic containing ZnO, 3: glass–ceramic containing CuO, 4: glass–ceramic containing SrO, **a** before immersion, **b** after immersion

identified to be compact with the appearance of some rounded crystalline structures.

(c) The glass–ceramic doped with CuO shows microcrystalline features more interlinked than the surrounding peripheries and seems to be separated by circular vitreous features. After immersion, the whole texture is wholly microcrystalline leaving in between some vitreous boundaries

(d) The glass–ceramic doped with SrO shows microcrystalline features similar to that identified in the undoped glass–ceramic. After immersion, the texture is observed to be of microcrystalline texture leaving some non-uniform remnant of vitreous boundaries.

After immersion in the phosphate solution, the following variations are reached:

1. The identified microcrystalline features remain as before immersion with the formation of additional rounded- or nodular-shaped microcrystalline phases.

2. The formed nodular-shaped microcrystals are not separately identified as been identified in references such as Hench's bioglass.

Discussion

Interpretation of the FT infrared absorption spectra of the studied glasses and glass–ceramics

The FT infrared spectral data of the studied glasses can be explained on the following basic parameters [10–20]:

1. It is recognized and universally accepted that the FTIR spectral bands and peaks represent the detailed structural building units within the glasses or in other words to be fingerprints of them [16, 17]. The structural building groups are responding to the abundance of the structural glass-forming oxides together with their arrangements in the glass network.
2. The basic chemical composition of the host glass is main (P_2O_5 (60) beside SiO_2(10)–Na_2O(20)–CaO(10) wt%). It is expected, therefore, that the main structural units are of phosphate groups (PO_4) together with additional secondary silicate groups (SiO_4) and the rest component oxides of Na_2O and CaO are situated in modifying positions.
3. The previous expectation indicates that the vibrating structural modes belong to main phosphate groups and with interfering of some silicate groups leading to condensed or compact IR mid-structure where the characteristic wavenumber positions of the two structural units are within nearby locations. According to the free independent vibrations concept adopted by Tarte [21] and Condrate [22], the two mixed main phosphate and silicate groups are free to vibrate in their specific wavenumber positions and the net result is the identified compact and extended vibrational peaks specifically in the mid-region extending from 400 to 1700 cm^{-1}.
4. It is therefore found necessary to apply a deconvolution process for the expected hidden or overlapped peaks in the studied base soda–lime silicophosphate host glass and its glass–ceramic derivatives (Figs. 8, 9) to interpret and assign the origin of the identified vibrational peaks.

Based on previous considerations, the FTIR data of the studied glasses can thus be interpreted as follows [13–20];

1. The far-IR peaks at 453, 505 and 545 cm^{-1} can be related mainly to bending vibrations of (O–P–O), (P=O) and some sharing of bending vibrations of Si–O–Si and O–Si–O.
2. The peaks at 702 and 785 cm^{-1} can be assigned to symmetric stretching vibrations of P–O–P rings or bridging γ_s(P–O–P) and some sharing of symmetric stretching of Si–O–Si.
3. The peaks at 872 and 1030 cm^{-1} can be correlated with an asymmetric stretch of (P–O–P) bridges in metaphosphate configurations, $\gamma_{as}(PO_2)$.
4. The peak at 1102 cm^{-1} is related to the asymmetric stretch of (P–O–P) in pyrophosphate groups $(PO_3)^{-2}$, the asymmetric stretch of PO_2 groups and sharing of Si–O stretching.
5. The peak at 1285 cm^{-1} is related to stretching vibrations of doubly bonded oxygen (P=O).
6. The peak at 1390 cm^{-1} is related to (PO_2) asymmetric stretching vibrations of metaphosphate groups.
7. The peaks at 1460 and 1627–1685 cm^{-1} are related to vibrations of carbonate, water and OH groups, respectively.
8. The near-IR peaks at 2846, 2925 cm^{-1} and the subsequent broadband centered at 3443 cm^{-1} are correlated with water, OH, POH, SiOH vibrations.

Interpretation of the effect of immersion in phosphate solution on the FTIR spectra

The changes in the FTIR of the studied phosphate glasses and glass–ceramics upon immersion in phosphate solution can be understood and interpreted on the following basis;

1. It has been recognized from the early invention of patented Hench's bioglass that the term bioactive candidate has been introduced and referred to biomaterials which upon immersion in fluids or some related solutions produce a specific surface material (hydroxyapatite) which is chemically bonded to bones and related tissues [23]. The first immersion process began with tris solution and then with simulated body fluid (SBF) as proposed by KoKubo and Takadama [24]. Day et al. [25, 26] have investigated the action of diluted phosphate solution through in vitro bioactivity studies on borate and borosilicate glasses. For dental applications, some authors studied the comparative immersion of Hench's bioglass in artificial saliva [27, 28].
2. The corrosion behavior of Hench's bioglass and derived glasses by different aqueous solutions has indicated that [29] the sodium phosphate solution is more corrosive than the action of solutions of acids, alkali hydroxide and even the other constituents in the SBF fluid. This behavior has been related to the ionization of the sodium phosphate solution into sodium hydroxide and phosphoric acid solutions dissolving nearly all the constituents of Hench's bioglass (silicate or phosphate phases).

3. Based on previous considerations, it is concluded that upon the immersion of the studied silicophosphate glasses, it is assumed that the glass undergoes specific surrounding reactions including the main phosphate and partner silicate phases with the phosphate solution and subsequently an HA-like layer is formed.
4. It is agreed that the formation of a hydroxyapatite layer is an important factor to decide the biological activity of a biomaterial in vitro [1–5].
5. It is accepted that the generation or identification of the far and other IR vibrational peaks at 560–605, 750 and related band at 1000–1100 cm^{-1} which indicate or point out the formation of calcium phosphate crystalline phase are clues for the formation of calcium phosphate as indication parameters for bioactivity.

Interpretation of the X-ray diffraction patterns data

The experimental X-ray data reveal variable crystalline phases within the prepared heat-treated four glass–ceramics which are dependent on the chemical composition of the glass and the type of dopants introduced before heat treatment. These crystalline data are explained based on the following parameters:

1. The chemical composition of the host undoped glass–ceramic under study consists of main P_2O_5(60) and with Na_2O(20), SiO_2(10) and CaO(10) wt%
2. McMillan [30] assumed that there is obvious evidence that the addition of a few percents of P_2O_5 in glasses promotes the presence of phase separation and subsequent ease of crystallization. Also, the double bond oxygen, P=O, is assumed to be a favorable promoter to phosphate phase separation in a silicate network and thus increases the tendency toward crystallization [31]. In the present studied glass–ceramic, the chemical composition of the parent glass contains major constituent of P_2O_5 (60%) and hence there are much phosphate ions and greater tendency to produce varieties of crystalline phosphates with the sharing of alkali oxide (Na_2O) and alkaline earth oxide (CaO).
3. Also, Hudon and Baker [32] have studied the readiness of various cations to produce nucleation sites and hence subsequently form crystalline phases and confirm that Ca^{2+} ions can participate and initiate phase separation and subsequent crystallization.

4 The X-ray diffraction data indicate that the undoped glass–ceramic contains six crystalline phases, three of which are of silicate phases from sodium calcium silicate, wollastonite (calcium silicate), grumantite (sodium silicate hydrated and suolunite (calcium silicate hydrated) with total 50.1% and two phosphate phases (sodium hydrogen phosphate and sodium phosphate) with 49.9%.

5. The previous result seems to be amazing and unpredictable because of the presence of P_2O_5 as the main component in the chemical composition of the base glass. It is assumed that P_2O_5 behaves in the suggested process or sequence of crystallization of the parent undoped glass at least partly as a nucleating agent for the separation of silicate phases as its role in the crystallization of Hench's bioglass into main sodium calcium silicate ($1Na_2O.\ 2CaO.\ 3SiO_2$) crystalline phase. Also, P_2O_5 is assumed to share in the production or formation of two crystalline phosphate phases with Na_2O. The calcium ions are consumed in the preparation of three silicate phases (sodium calcium silicate, wollastonite ($CaSiO_3$) and calcium silicate hydrated.
6. The glass–ceramic doped with ZnO shows only three crystalline phosphates of calcium, zinc and sodium. This result indicates that ZnO conducts or initiates the separation of phosphate phase according to the assumption of Hudon and Baker [32] and the remaining connecting vitreous boundary is assumed to contain silica in its constitution.
7. The glass–ceramic doped with CuO consists of two crystalline phosphate phases with sodium and calcium with a total of 73.6%, and the rest are two copper phosphates crystalline phases. The role of CuO can be assumed to conduct a catalytic effect for the formation of the different phosphates besides the sharing of the formation of two copper phosphates.
8. The last glass–ceramic doped with SrO comprises three crystalline phosphates of calcium and two sodium with major constituents (~96.2%), and SrO is observed to share in forming a limited crystalline phase of sodium strontium phosphide (3.8%). This may be related or assumed to some residence of Sr ions in close-packing sites and have not freedom of choice to react or combine with phosphate anions directly.
9. In conclusion, the collected X-ray diffraction data reveal peculiar results in which the undoped glass–ceramic is identified to contain almost equal crystalline phases of silicate and phosphate irrespective of the main constituent of P_2O_5 (60%). On the other hand, the three doped glasses reveal only different crystalline phosphate phases with partly sharing of the dopant oxide and with no crystalline silicate phases. These results can be assumed to the tendency of P_2O_5 acting as nucleating or initiating phase separation and the preference of combination of P_2O_5 to form crystalline phosphates and leaving the silica component in surrounding vitreous matrix. These results seem to need further studies to find out the preference combination and subsequent crystallization process.

Interpretation of the scanning electron microscopic and EDAX data

Figures 9 and 10 illustrate the SEM and EDAX results of the four glass–ceramic samples before and after immersion in phosphate solution. The micrographs show multi- and microcrystalline phases covering nearly all the surfaces with remnants of the in-between vitreous matrix. These extended features of microcrystalline features are related to the presence of multicomponent phosphates and silicate crystalline phases identified in the various four glass–ceramics and even the base undoped glass–ceramic which consists of different six phosphate and silicate phases. Such identified phases are originating from the sharing of all the constitutional oxides during the process of crystallization. In the other three doped glass ceramics, all the formed crystalline phases are from different phosphate phases with the combinations of the partner's sodium or calcium. This result points out that the additions of the studied three dopants (ZnO, SrO, CuO) retard the formation of any crystalline silicate phases but easily combine with P_2O_5 as a preferred partner. This specific behavior seems to be in need of further successive studies.

On the other hand, EDAX data indicate the appearance of main (P) beside the other commonest constituents Na, Ca, but Si is absent to be detected only in the undoped glass–ceramic. This may be related to the strong combination of the Si species in three formed microcrystalline formed phases.

The overall SEM data indicate that the studied glasses after immersion in phosphate solution reveal some nodular-shaped microcrystalline phases but not highly distinct as identified for reference bioactive glasses such as Hench's bioglass due to the following reasons:

1. The host glass contains P_2O_5 with 60% which initiates the formation of many microcrystalline phases of phosphates beside some silicate phases referring to the tight bonding of P_2O_5 in its crystalline phases.
2. The presence of CaO with 10% of the composition and the calcium ions are assumed to form microcrystalline phosphates, silicates and are not free to form calcium phosphate except in the scattered identified rounded semi-or nodular microcrystalline phases.

Conclusions

In this study, the synthesis of base Na–Ca–silicophosphate glass of the composition ($60P_2O_5$–$10SiO_2$–$20Na_2O$–10CaO wt%), together with samples doped with 2%ZnO, 1%CuO or 2%SrO, was prepared by melting and annealing technique. Samples of glasses were thermally heat-treated in a two-step regime to convert them to their corresponding glass–ceramics. X-ray diffraction data of the undoped glass–ceramic indicate the appearance of equal three phosphate crystalline phases together with three silicate phases. The doped glasses reveal mostly different crystalline phases from phosphates only as assumed by initiating phase separation of the different dopant oxides. FTIR spectra of the glasses and their glass–ceramics before and after immersion in the phosphate solution were carried out to identify the structural building groups and searching for any variations after immersion. FTIR results refer to the generation of multicomponent far-IR peaks at 400–750 cm^{-1} after immersion which supports bioactivity behavior.

SEM images of the glass–ceramics before and after immersion show multi-microcrystalline phases which vary with the dopant oxide. After immersion, the SEM data reveal the formation of some nodular or rounded microcrystalline phases but not highly distinctive as with bioactive Hench's bioglass. This behavior has been related to the difference in the percents of high P_2O_5 (60%) which initiates the generation of multi-crystalline phases of different structures and compositions and the calcium ions are assumed to be firmly bonded in their crystalline phases and their reaction with P_2O_5 to form hydroxyapatite is limited. The data show no distinct variation of the dopants on the bioactivity behavior.

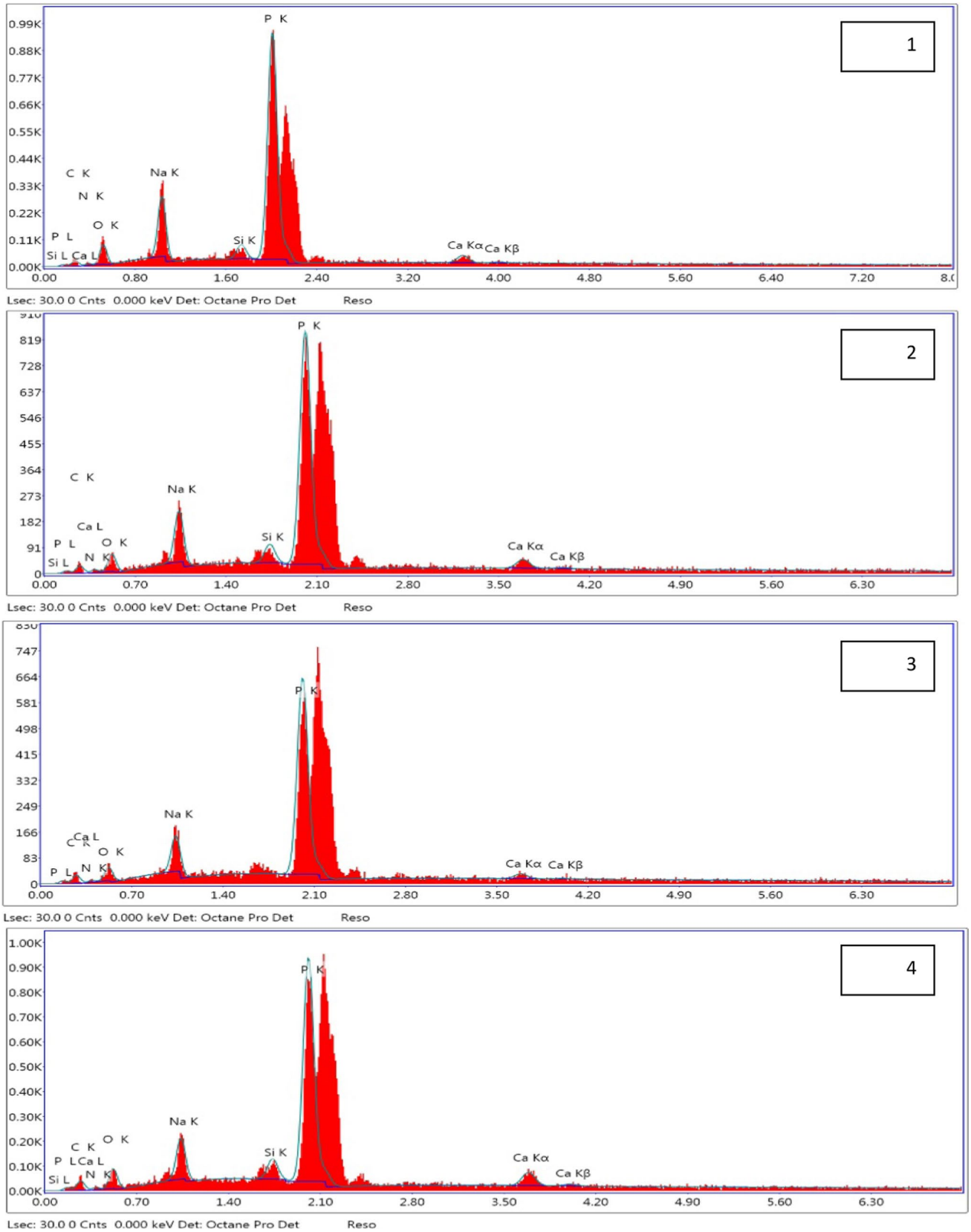

Fig. 10 EDAX analysis of glass samples after immersion in phosphate solution for 2 weeks, 1: base glass, 2: glass containing ZnO, 3: glass containing CuO and 4: glass containing SrO

Acknowledgements The authors of this work wish to express their gratitude to the authorities of National Research Centre, Egypt, for their financial support to conduct this work under the Project No. 11090314.

References

1. Hench, L.L.: The story of Bioglass. J. Mater. Sci. Mater. Med. **17**, 967–978 (2006)
2. Jones, J.R.: Review of bioactive glass: from Hench to hybrids. Acta Biomater. **9**, 4457–4486 (2013)
3. Hench, L.L.: Bioceramica. J. Am. Ceram. Soc. **81**(7), 1705–1728 (1998)
4. Abdelghany, A.M., ElBatal, H.A., EzzElDin, F.M.: Bone Bonding ability behavior of some ternary borate glasses by immersion in sodium phosphate solution. Ceram. Int. **18**, 1105–1113 (2012)
5. Marzouk, M.A., ElBatal, H.A.: In vitro bioactivity of soda-lime borate glasses with substituted SrO in sodium phosphate solution. Process. Appl. Ceram. **8**(3), 167–177 (2014)
6. White, J.E., Brown, R.F., McMenamin, K.D.: Transformation of borate glasses into biologically useful materials. Glass Technol **44**(2), 75–81 (2003)
7. Day, D.E.: Conversion Kinetics of silicate, Borosilicate and borate bioactive glasses, hydroxyapatite. Phys. Chem. Glasses Eur. J. Glass Sci. Technol. (B) **50**(2), 85–88 (2009)
8. Deliormanh, A.M., Vatansever, H.S., Yesil, H., OzdabKurt, F.: In vivo evaluation of cerium, gallium and vanadium-doped borate-based bioactive glass Scaffolds using rat subcutaneous implantation model. Ceram. Int. **42**, 11574–11583 (2016)
9. ElBatal, F.H., ElKheshen, A.A., El-Bassyouni, G.T., Abdel-Aty, A.A.: In vitro Bioactivity Behavior of some Borate Glasses and their glass–ceramic derivatives containing Zn^{2+}, Ag^{+} or Cu^{2+} by immersion in phosphate solution and their anti-microbial activity. Silicon (2017). https://doi.org/10.1007/s12633-017-9552-y
10. Abdel-Kader, A., Higazy, A.A., ElKholy, M.M.: Compositional dependence of infrared absorption spectra studies for TeO_2–P_2O_5 and TeO_2–P_2O_5–Bi_2O_3 glasses. J. Mater. Sci. Mater. Electron. **2**, 137 (1991)
11. Moustafa, Y.M., El-Egili, K.: Infrared spectra of sodium phosphate glasses. J. Non Cryst. Solids **240**, 144 (1998)
12. ElBatal, F.H., Marzouk, M.A., Abdelghany, A.M.: UV–visible and infrared absorption spectra of gamma irradiated V_2O_5-doped in sodium phosphate, lead phosphate, zinc phosphate glasses: a comparative study. J. Non Cryst. Solids **357**, 102 (2011)
13. Husung, R.D., Doremus, R.H.: The infrared transmission spectra of four silicate glasses before and after exposure to water. J. Mater. Res. **5**(10), 2209 (1990)
14. AboNaf, S.M., ElBatal, F.H., Azooz, M.A.: Characterization of some glasses in the system SiO_2, Na_2O· RO by infrared spectroscopy. Mater. Chem. Phys. **77**, 846 (2003)
15. ElBatal, H.A., Azooz, M.A., Saad, E.A., EzzElDin, F.M., Amin, M.S.: Corrosion behavior mechanism of borosilicate glasses towards different leaching solutions evaluated by the grain method and FTIR Spectral analysis before and after gamma irradiation. Silicon (2012). https://doi.org/10.1007/s12633-017-9586-1
16. Wong, J., Angell, C.A.: Glass Structure by Spectroscopy. Marcel Dekker, New York (1976)
17. Efimov, A.M.: IR fundamental spectra and structure of pyrophosphate glasses along the $2ZnO{\cdot}P_2O_5$–$2Me_2O{\cdot}\ P_2O_5$ join (Me being Na and Li). J. Non Cryst. Solids **209**, 209 (1997)
18. Metwalli, E., Karrabul, M., Sidebottom, D.L., Morsi, M.M., Brow, R.K.: Properties and structure of copper ultraphosphate glasses. J. Non Cryst. Solids **344**, 128 (2004)
19. El-Batal, F.H.: Gamma-ray interaction with copper-doped sodium phosphate glasses. J. Mater. Sci. **43**(3), 1036 (2008)
20. Marzouk, M.A., Hamdy, Y.M., ElBatal, H.A.: Photoluminescence and spectral performance of manganese ions in zinc phosphate and barium phosphate host glasses. J. Non Cryst. Solids **458**, 1 (2017)
21. Tarte, P.: Identification of Li–O bands in the infra-red spectra of simple lithium compounds containing LiO_4 tetrahedra. Spectrochim. Acta **20**, 238 (1964)
22. Condrate R.A.: Introduction to glass science. Pye, L.D., Stevens, H.J., LaCourse, W.C. (eds.) The Vitreous State Plenum Press, New York, p. 101 (1972)
23. Hench, L.L., Splinter, R.J., Allen, W.C., Greenlee, T.K.: Bonding mechanisms at the interface of ceramic prosthetic materials. J. Biomed. Mater. Res. **5**(6), 117 (1971)
24. Kokubo, T., Takadama, H.: How useful is SBF in predicting in vivo bone bioactivity? Biomaterials **27**, 2907–2915 (2006)
25. Day, D.E., White, J.E., Brown, R.F., McMenamin, K.D.: Transformation of borate glasses into biologically useful materials. Glass Technol. **44**(2), 75–81 (2003)
26. Huang, W., Day, D.E., Kittiratanapiboon, K., Ruhman, M.N.: Kinetics and mechanisms of the conversion of silicate (45S5), borate, and borosilicate glasses to hydroxyapatite in dilute phosphate solutions. J. Mater. Med. **17**(7), 583–596 (2006)
27. Plewinski, M., Chickle, K.S., Lindener, M., Kirsten, A., Weber, M., Fisher, H.: The effect of crystallization of bioactive bioglass 45S5 on apatite formation and degradation. Dent. Mater. **29**, 1256–1264 (2013)
28. Aina, V., Bertinetti, L., Cerrato, G., Cerruti, M., Lusvardi, G., Malavasi, G., Menabue, L.: On the dissolution/reaction of small-grain Bioglass® 45S5 and F-modified bioactive glasses in artificial saliva (AS). Appl. Surf. Sci. **257**(9), 4185 (2011)
29. Elbadry, K.M., Moustafa, F.A., Azooz, M.A., ElBatal, F.H.: Corrosion behaviour of some selected bioglasses by different aqueous solutions. Glass Technol. **43**(4), 162–170 (2002)
30. McMillan, P.W.: Glass-Ceramics, 2nd edn. Academic Press, London (1979)
31. Peitl, O., Znotto, E.D., Hench, L.L.: Highly bioactive P_2O_5–Na_2O–CaO–SiO_2 glass–ceramics. J. Non Cryst. Solids **292**, 115–126 (2001)
32. Hudon, P., Buker, D.R.: The nature of phase separation in binary oxide melts and glasses. II. Selective solution mechanism. J. Non Cryst. Solids **303**(3), 346–353 (2002)